Precision limit for simultaneous phase and transmittance estimation with phase-shifting interferometry

Ryo Okamoto and Tatsuki Tahara

Phys. Rev. A **104**, 033521 — Published 22 September 2021

DOI: 10.1103/PhysRevA.104.033521

Precision limit for simultaneous phase and transmittance estimation with phase shifting interferometry

Ryo Okamoto[1,2,*] and Tatsuki Tahara[3,2]

[1]*Department of Electronic Science and Engineering, Kyoto University, Kyoto Daigaku-Katsura, Nishikyo-ku, Kyoto 615-8510, Japan*
[2]*PRESTO, Japan Science and Technology Agency, 4-1-8 Honcho, Kawaguchi, Saitama 332-0012, Japan*
[3]*Applied Electromagnetic Research Center, Radio Research Institute, National Institute of Information and Communications Technology (NICT), 4-2-1 Nukuikitamachi, Koganei, Tokyo 184-8795, Japan*

(Dated: August 5, 2021)

The use of phase shifting interferometry (PSI) in the ultra-low light region would open the way for important applications, such as imaging of phototoxic substances and sensing of ultrafast phenomena. In the ultra-low light region, the statistical nature of photons can be a dominant source of noise compared with other noise caused by experimental instruments. Here, we theoretically derive the precision limit determined by the statistical nature of photons for simultaneously measuring the transmittance and phase of a sample with PSI. We show that the precision of PSI depends on the phase and transmittance themselves. We also show a trade-off relation between transmittance and phase. Then, we compare PSI with sequential optimal measurements in which the transmittance and phase of a sample are separately measured for each corresponding optimal measurement. We also discuss the case where the input number of photons fluctuates with a Poisson distribution and show that the fluctuation affects both the transmittance and phase precision for PSI.

PACS numbers:

I. INTRODUCTION

Phase shifting interferometry (PSI) is a powerful and well established technique to measure the phase and transmittance of a sample [1], widely used for various applications, such as optical surface quality measurements [1, 2], quantitative phase microscopy [3–7] and digital holography [8–14]. In PSI, a phase shifter is placed on one arm of an interferometer and a sample is placed on the other arm, and the output light intensities of the interferometer are measured for several reference phases added by the phase shifter. The transmittance and phase of the target are estimated from these measured intensities.

Recently, PSI has been applied to measurements at the photon-counting level [15, 16]. The use of PSI in the ultra-low light region would open the way for important applications, such as the imaging of cells containing phototoxic molecules and the measurement of ultrafast phenomena. In the ultra-low light region, the statistical nature of photons can be a dominant source of noise compared with noise caused by experimental instruments. Consequently, it is important to understand the effect of noise caused by the statistical nature of photons in PSI.

In a pioneering study, Yamamoto *et al.* experimentally observed how the measurement precision in digital holography using PSI is affected by the statistical nature of photons [15]. The experiment was performed at the photon-counting level using a weak coherent light and a photon detector. PSI was used to estimate the phase shift caused by a sample and the precision of the estimated phase was evaluated from the experimental data. In another study, a numerical simulation of digital holography taking into account the Poisson fluctuation of input photon number was conducted to evaluate the precision of transmittance estimates using PSI [17]. Recently, the precision of phase measurement for PSI has been theoretically derived by considering the fluctuation of photo-generated electrons in a photodetector, but the input light was assumed to have no statistical nature [18]. Thus, the fundamental precision limit determined by the statistical nature of photons for PSI has not yet been theoretically derived.

In this paper, we theoretically derive the precision limit when estimating the transmittance and phase for a sample with PSI. We find that the measurement precision for transmittance and phase depends on the unknown transmittance and phase themselves. A trade-off relation between transmittance and phase is also observed. Then, we compare PSI with sequential optimal measurements (SOM) in which the transmittance and phase of a sample are separately

*Electronic address: okamoto.ryo.4w@kyoto-u.ac.jp

measured for each corresponding optimal measurement for single photon inputs. While the transmittance estimation used in standard PSI gives a slightly worse precision than that for SOM, an alternative approach, which is not commonly used in PSI, almost reaches the precision for SOM. Regarding the phase estimation, we show that PSI can achieve a better precision than SOM. We also discuss the case where the input number of photons fluctuates with a Poisson distribution. We show that the input photon number fluctuation affects both the transmittance and phase precision for PSI and the dependence on the phase disappears.

This paper is organized as follows. In section 2, we define the precision for SOM. In section 3, we theoretically derive the precision for PSI and then numerically analyze and compare the performance. Section 4 concludes the paper.

II. PRECISION FOR SEQUENTIAL OPTIMAL MEASUREMENTS OF TRANSMITTANCE AND PHASE

In this section, we define the measurement precision for SOM. In the following sections, we compare the precision for SOM with that for PSI. If one is interested in only the transmittance of a sample, combining a single-photon state as an input with photon counting detection just after the sample gives the optimal precision at the ultimate quantum limit beyond the classical limit (shot-noise limit) [19, 20], although it is completely insensitive to the phase of the sample. On the other hand, if one is interested in only the phase of the sample, the standard interferometric limit gives the best precision for phase measurement with single photon inputs [21]. For simplicity, we assume N input photons divided into $N/2$ photons for each measurement. Thus, when we sequentially estimate the transmittance T and phase ϕ for a sample with each optimal measurement, the uncertainties of the transmittance $\Delta T_{\rm S}$ and phase $\Delta\phi_{\rm S}$ for SOM are given as follows [19–21]:

$$\Delta T_{\rm S} = \frac{1}{\sqrt{N}}\sqrt{2T(1-T)} \tag{1}$$

$$\Delta\phi_{\rm S} = \frac{1}{\sqrt{N}}\frac{1+\sqrt{T}}{\sqrt{2T}}. \tag{2}$$

III. PRECISION FOR SIMULTANEOUS MEASUREMENT OF TRANSMITTANCE AND PHASE WITH PSI

In this section, we theoretically derive the precision for PSI. Figure 1 shows a schematic of PSI. First, photons are input into a beam splitter (BS1) and are divided into two paths. Then, the photons pass through the phase shifter (PS) in one of the paths and through the sample having transmittance T and phase $\phi_{\rm m}$ in the other path. After being recombined at a second beam splitter (BS2), the photons are detected at the output by two single-photon detectors (SPD1 and SPD2). Note that we assume that the single photon detectors have a perfect detection efficiency and no dark count in order to focus on the precision limit given by the statistical nature of the photons.

For a reflectivity of the first beam splitter (BS1) of r and that of the second (BS2) of 50%, the probability that a photon is detected by SPD1 can be written as follows:

$$p(\theta) = \frac{1}{2}\left(1 - r(1-T) + 2\sqrt{Tr(1-r)}\cos(\phi_{\rm m} - (\theta_{\rm off} + \theta))\right), \tag{3}$$

where $\theta_{\rm off}$ and θ are the offset phase of PS and the phase shift given by PS, respectively. The probability that a photon is detected by SPD2 is $p(\theta+\pi)$. Therefore, when N photons are input into the setup, the photon counts detected by SPD1 and SPD2 are given by $N \times p(\theta)$ and $N \times p(\theta+\pi)$, respectively.

Different versions of PSI use different numbers of steps for the phase shift. In this paper, we focus on four-step PSI, which is most widely used. When photons are detected at both outputs, we can obtain four kinds of counts corresponding to the required four phases from just two phases (0 and $\pi/2$) of the PS. We assume that the total input photon number N is distributed equally over the two phase shifts. Thus, the four kinds of photon counts are written as $N_i \equiv N/2 \times p_i$, where $p_i \equiv p((i-1)\pi/2)$ and $i = 1, 2, 3, 4$. The transmittance and phase can be extracted as follows:

$$T = \frac{1}{N^2 r(1-r)}(N_{24}^2 + N_{13}^2) \tag{4}$$

$$\phi = \arctan\frac{N_{24}}{N_{13}}, \tag{5}$$

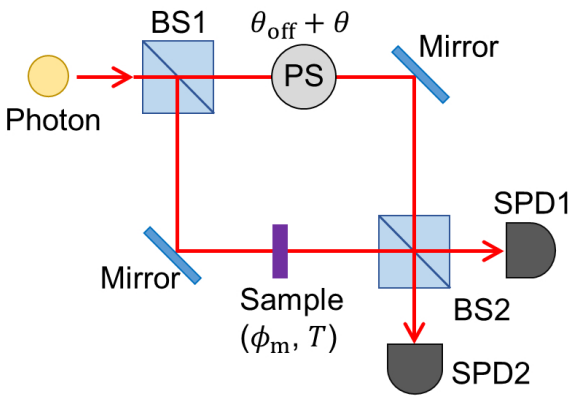

FIG. 1: Schematic of PSI. Photons are input into the interferometer. The phase ($\phi_{\rm m}$) and transmittance (T) for the sample are measured through the detection of the photons with single-photon detectors (SPD1 and SPD2) at the output. The phase shifter (PS) is used to control the phase of the interferometer. BS: beam splitter. $\theta_{\rm off}$: offset phase of PS. θ: phase shift given by PS.

where $\phi \equiv \phi_{\rm m} - \theta_{\rm off}$, $N_{13} \equiv N_1 - N_3$ and $N_{24} \equiv N_2 - N_4$. Since $\theta_{\rm off}$ can be determined by an independent measurement, we can obtain the phase for the sample $\phi_{\rm m}$. We also consider another approach to estimate T from the photon counts as follows:

$$T = \sqrt{\frac{4}{r^2N^2}(N_1^2+N_2^2+N_3^2+N_4^2) + 3\left(\frac{1-r}{r}\right)^2} - 2\frac{1-r}{r}. \tag{6}$$

Although this is not commonly used in PSI, the precision for the transmittance estimated from Eq. (6) can be higher than that estimated from Eq. (4), as we will show in the following analysis.

First, we consider the case where the number of photons used is constant for each measurement. This corresponds to the situation in which N photons from a single photon source are used for each measurement. In this case, the variance of the detected photon count is given by $\Delta N_i^2 = \frac{N}{2}p_i(1-p_i)$. We also took into account the covariance between N_1 and N_3 and between N_2 and N_4, which are given by ${\rm Cov}(N_i, N_j) = -\frac{N}{2}p_ip_j$ ($\{i,j\} = \{1,3\}$ or $\{2,4\}$). The uncertainties of the estimated transmittance, $\Delta T_{\rm PS}$ and $\Delta T_{\rm PS'}$, and phase $\Delta\phi_{\rm PS}$ are obtained using Eqs. (4), (6) and (5), respectively, through an error propagation analysis as follows:

$$\Delta T_{\rm PS} = \frac{1}{\sqrt{N}}\sqrt{\frac{2T(1-r-(2-3r)rT - r(1-r)T\cos(4\phi))}{r(1-r)}} \tag{7}$$

$$\Delta T_{\rm PS'} = \frac{1}{\sqrt{N}}\sqrt{\frac{(1-r)^3+(1-r)^2(1+8r)T - r(1-r)(11-20r)T^2 - r^2(7-8r)T^3 - r^3T^4 - 2r(1-r)^2T^2\cos(4\phi)}{r(2+r(T-2))^2}} \tag{8}$$

$$\Delta\phi_{\rm PS} = \frac{1}{\sqrt{N}}\sqrt{\frac{1-r+r^2T+r(1-r)T\cos(4\phi)}{2r(1-r)T}}. \tag{9}$$

These equations show that all uncertainties depend on T and ϕ in a nontrivial manner. Equation (8) indicates that $\Delta T_{\rm PS'}$ is minimized when $r = 1$ and reaches the quantum limit for an N photon input: $\Delta T_{\rm PS'} = \frac{1}{\sqrt{N}}\sqrt{T(1-T)} = \Delta T_{\rm S}/\sqrt{2}$. However, in this case, $\Delta T_{\rm PS}$ and $\Delta\phi_{\rm PS}$ diverge to infinity.

We find that both $\Delta T_{\rm PS}$ and $\Delta\phi_{\rm PS}$ will be minimized when r satisfies the relation $r = \frac{1}{1+\sqrt{T}}$. Note that this relation is also required to achieve the standard interferometric limit [21]. After substituting this relation into Eqs. (7), (8) and (9), we obtain the following equations:

$$\Delta T_{\rm PS} = \frac{1}{\sqrt{N}}\sqrt{2T\left(1+2\left(\sqrt{T}-T\right)-T\cos(4\phi)\right)} \tag{10}$$

$$\Delta T_{\rm PS'} = \frac{1}{\sqrt{N}}\frac{\sqrt{\sqrt{T}+9T+10\sqrt{T}T-10T^2-7\sqrt{T}T^2-T^3-2T^2\cos(4\phi)}}{2+\sqrt{T}} \tag{11}$$

$$\Delta\phi_{\rm PS} = \frac{1}{\sqrt{N}}\sqrt{\frac{1+2\sqrt{T}+T\cos(4\phi)}{2T}}. \tag{12}$$

Equations (10) and (11) show that $\Delta T_{\rm PS}$ and $\Delta T_{\rm PS'}$ are minimized for a given T when the phase ϕ satisfies $\cos(4\phi) = 1$. In this case, $\Delta T_{\rm PS} = \Delta T_{\rm PS'} = \Delta T_{\rm S} = 0$ at $T = 1$. At $T = 0$, $\Delta T_{\rm PS} = \Delta T_{\rm PS'} = \Delta T_{\rm S} = 0$ with arbitrary ϕ. Equation (12) shows that $\Delta\phi_{\rm PS}$ is equal to or smaller than $\Delta\phi_{\rm S}$. $\Delta\phi_{\rm PS}$ is minimized for a given T when the phase ϕ satisfies $\cos(4\phi) = -1$. In this case, when $T = 1$, $\Delta\phi_{\rm PS}$ reaches the standard quantum limit $1/\sqrt{N}$ for an N photon input. $\Delta\phi_{\rm PS}$ is maximized and is equal to $\Delta\phi_{\rm S}$ when the phase ϕ satisfies $\cos(4\phi) = 1$.

Figures 2(a) and 2(c) illustrate $\Delta T_{\rm PS}$ and $\Delta T_{\rm PS'}$ for $N = 100$, respectively. In Figs. 2(b) and 2(d), we compare $\Delta T_{\rm PS}$ and $\Delta T_{\rm PS'}$ with $\Delta T_{\rm S}$ for ϕ satisfying $\cos(4\phi) = 1$ (orange dashed curve) and $\cos(4\phi) = -1$ (red dot-dashed curve). The blue solid curves in Figs. 2(b) and 2(d) correspond to $\Delta T_{\rm S}$. $\Delta T_{\rm PS}$ and $\Delta T_{\rm PS'}$ depend on ϕ except for at $T = 0$. For ϕ satisfying $\cos(4\phi) = 1$, both $\Delta T_{\rm PS}$ and $\Delta T_{\rm PS'}$ are 0 at $T = 0$ and 1. $\Delta T_{\rm PS}$ and $\Delta T_{\rm PS'}$ have different maximum values of 0.096 at $T = 0.53$ and 0.077 at $T = 0.47$, respectively. $\Delta T_{\rm PS'}$ almost reaches $\Delta T_{\rm S}$ while $\Delta T_{\rm PS}$ is maximally 37% larger than $\Delta T_{\rm S}$. When ϕ satisfies $\cos(4\phi) = -1$, $\Delta T_{\rm PS}$ monotonically increases with T, reaching a maximum value of 0.2 at $T = 1$, while $\Delta T_{\rm PS'}$ has a maximum value of 0.087 at $T = 0.59$ and has a slightly smaller value of 0.067 at $T = 1$. The comparison between $\Delta T_{\rm PS}$ (Fig. 2(b)) and $\Delta T_{\rm PS'}$ (Fig. 2(d)) reveals that the T estimation with Eq. (6) allows a higher precision than that with Eq. (4) except for the region around $0 < T < 0.1$.

Figure 2(e) illustrates $\Delta\phi_{\rm PS}$ for $N = 100$. In contrast to $\Delta T_{\rm PS}$, $\Delta\phi_{\rm PS}$ diverges to infinity at $T = 0$. As T increases, $\Delta\phi_{\rm PS}$ decreases and an oscillation with ϕ appears. Figure 2(f) shows $\Delta\phi_{\rm PS}$ when ϕ satisfies $\cos(4\phi) = 1$ (orange dashed curve) and $\cos(4\phi) = -1$ (red dot-dashed curve). The blue solid curve in Fig. 2(f) corresponds to $\Delta\phi_{\rm S}$. As

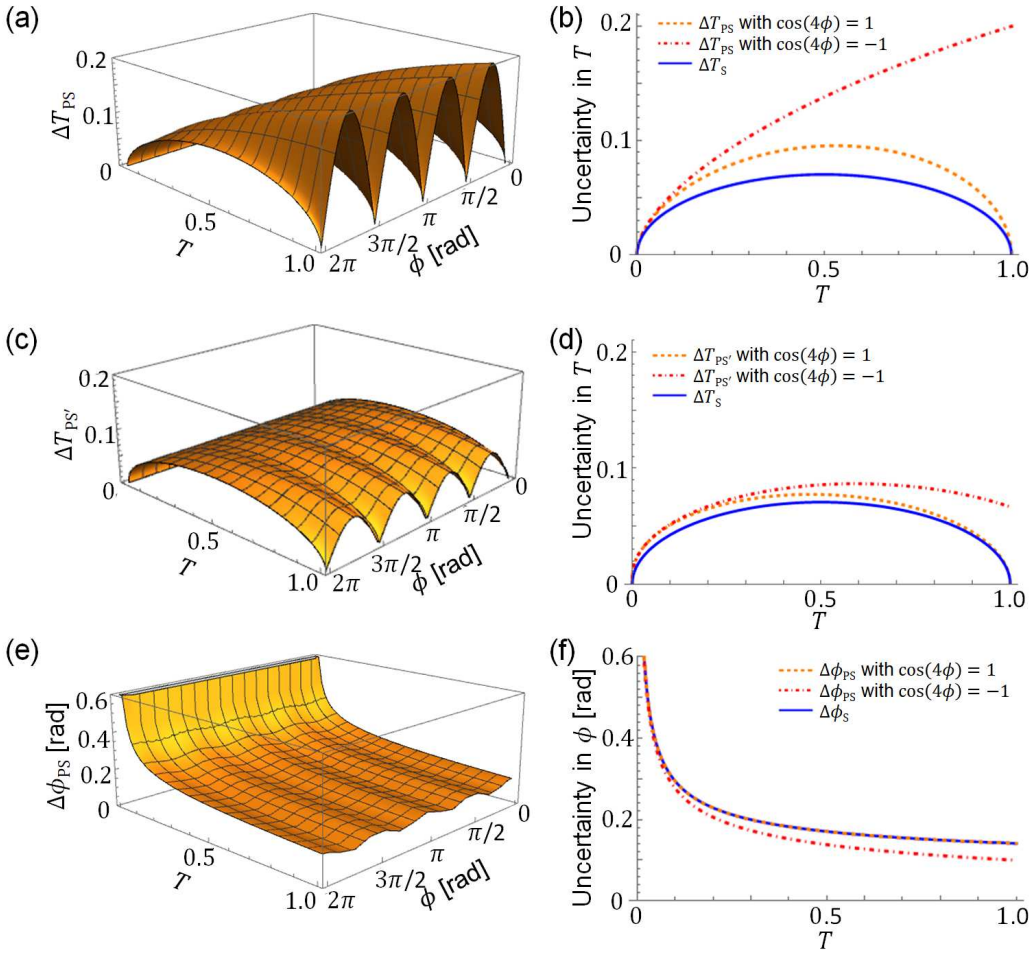

FIG. 2: Measurement uncertainties in the estimation using PSI for $N = 100$ input photons. (a)-(d): uncertainties in T. (a) and (c) illustrate $\Delta T_{\rm PS}$ and $\Delta T_{\rm PS'}$, respectively. In (b), the orange dashed and red dot-dashed curves indicate $\Delta T_{\rm PS}$ with $\cos(4\phi) = 1$ and $\cos(4\phi) = -1$, respectively. In (d), the orange dashed and red dot-dashed curves indicate $\Delta T_{\rm PS'}$ with $\cos(4\phi) = 1$ and $\cos(4\phi) = -1$, respectively. The blue solid curves in (b) and (d) indicate $\Delta T_{\rm S}$. (e), (f): uncertainties in ϕ. (e) illustrates $\Delta\phi_{\rm PS}$. In (f), the orange dashed and red dot-dashed curves indicate $\Delta\phi_{\rm PS}$ with $\cos(4\phi) = 1$ and $\cos(4\phi) = -1$, respectively. The blue solid curve indicates $\Delta\phi_{\rm S}$.

discussed above, $\Delta\phi_{\rm S}$ is equal to $\Delta\phi_{\rm PS}$ for ϕ satisfying $\cos(4\phi)=1$. When ϕ satisfies $\cos(4\phi)=-1$, $\Delta\phi_{\rm PS}$ reaches the standard quantum limit of $1/\sqrt{N}=0.1$ at $T=1.0$.

Comparing Figs. 2(a) and 2(c) with Fig. 2(e), we see that the values of ϕ minimizing $\Delta\phi_{\rm PS}$ maximize $\Delta T_{\rm PS}$ and $\Delta T_{\rm PS'}$, and vice versa. Also, for the T dependence, $\Delta\phi_{\rm PS}$ diverges to infinity at $T=0$ while $\Delta T_{\rm PS}$ and $\Delta T_{\rm PS'}$ take a minimum value of 0 at $T=0$. This suggests a trade-off between the uncertainties in the estimation of T and ϕ. Note that we can control $\theta_{\rm off}$ of PS to satisfy a desired condition (such as $\cos(4\phi)=1$) through the relation $\phi=\phi_{\rm m}-\theta_{\rm off}$. An adaptive strategy is available for this purpose even if we have no information about the target phase $\phi_{\rm m}$ [22–26]. Similarly, we can adaptively tune the reflectance of BS1 to be $r=\frac{1}{1+\sqrt{T}}$ using a tunable BS.

Next, we consider the case where the input photons have a Poisson distribution in photon number per unit time, and it affects the statistics of the output photons. This situation can occur in many conventional systems where a coherent light is used for the input and the photon number or power at the output is measured during an accumulation time. In this case, the Poisson fluctuation affects the variance of the detected photon count and changes it to $\Delta N_i^2=N_i p_i$ from $\Delta N_i^2=N_i p_i(1-p_i)$. The uncertainties of the estimated transmittance, $\Delta T_{\rm PSP}$ and $\Delta T_{\rm PSP'}$, and phase $\Delta\phi_{\rm PSP}$ are obtained using Eqs. (4), (6) and (5), respectively, through an error propagation analysis as follows:

$$\Delta T_{\rm PSP} = \frac{1}{\sqrt{N}}\sqrt{\frac{2T(rT+1-r)}{(1-r)r}} \tag{13}$$

$$\Delta T_{\rm PSP'} = \frac{1}{\sqrt{N}}\frac{\sqrt{(1-r)^3+9r(1-r)^2T+9r^2(1-r)T^2+r^3T^3}}{r(2+r(T-2))} \tag{14}$$

$$\Delta\phi_{\rm PSP} = \frac{1}{\sqrt{N}}\sqrt{\frac{rT+1-r}{2rT(1-r)}}, \tag{15}$$

Because the ϕ-dependent terms cancel each other in the derivation process, these uncertainties do not depend on ϕ but only on T, unlike $\Delta T_{\rm PS}$, $\Delta T_{\rm PS'}$ and $\Delta\phi_{\rm PS}$. Note that the cancellation of the ϕ-dependent terms is a feature that occurs specifically in four-step PSI. It does not occur, for instance, in three-step PSI. Equation (14) is minimized to be $\Delta T_{\rm PSP'}=\sqrt{T/N}$ when $r=1$. However, in this case, $\Delta T_{\rm PSP}$ and $\Delta\phi_{\rm PSP}$ diverge to infinity. Equations (13) and (15) are minimized when r satisfies the relation $r=\frac{1}{1+\sqrt{T}}$, which was also used to optimize Eqs. (7) and (9). After substituting this relation into Eqs. (13), (14) and (15), we obtain the following equations:

$$\Delta T_{\rm PSP} = \frac{1}{\sqrt{N}}\sqrt{2T}\left(1+\sqrt{T}\right) \tag{16}$$

$$\Delta T_{\rm PSP'} = \frac{1}{\sqrt{N}}\frac{1+\sqrt{T}}{2+\sqrt{T}}\sqrt{\left(1+T+8\sqrt{T}\right)\sqrt{T}} \tag{17}$$

$$\Delta\phi_{\rm PSP} = \frac{1}{\sqrt{N}}\frac{1+\sqrt{T}}{\sqrt{2T}}. \tag{18}$$

We can see that $\Delta\phi_{\rm PSP}$ is exactly the same as $\Delta\phi_{\rm S}$ and $\Delta\phi_{\rm PS}$ with $\cos(4\phi)=1$.

Figure 3(a) illustrates $\Delta T_{\rm PSP}$ (red dashed curve) and $\Delta T_{\rm PSP'}$ (purple dotted curve) when $N=100$. $\Delta T_{\rm PSP}$ and $\Delta T_{\rm PSP'}$ are 0 at $T=0$ and monotonically increase with T and have maximum values of about 0.28 and 0.21, respectively. These T dependences are similar to that for $\Delta T_{\rm PS}$ with $\cos(4\phi)=-1$ (red dot-dashed curve in Fig. 2(a)) but the maximum values are different. $\Delta T_{\rm S}$ is smaller than both $\Delta T_{\rm PSP}$ and $\Delta T_{\rm PSP'}$ and the difference is largest at $T=1$. Note that the input photons for SOM are assumed to be a single-photon state. Thus, when the input photons has a Poisson fluctuation, the uncertainty in T for the sequential strategy increases and has a similar shape to $\Delta T_{\rm PSP}$ and $\Delta T_{\rm PSP'}$. Note also that SOM has a drawback in practical implementation; it requires two separate experimental setups to measure the phase and transmittance of a sample.

Figure 3(b) shows $\Delta\phi_{\rm PSP}$ when $N=100$. $\Delta\phi_{\rm PSP}$ (red dashed curve) diverges to infinity at $T=0$ and decreases with T, reaching a minimum value of about 0.14 at $T=1$. As shown above, $\Delta\phi_{\rm PSP}$ is the same as $\Delta\phi_{\rm S}$ (blue solid curve in Fig. 3(b)).

Comparing Fig. 3(a) with Fig. 3(b), we see that the T minimizing $\Delta\phi_{\rm PSP}$ maximizes $\Delta T_{\rm PSP}$ and $\Delta T_{\rm PSP'}$, and vice versa. This suggests that there is a trade-off between the uncertainties in the estimation of T and ϕ also when the input photons have a Poisson fluctuation.

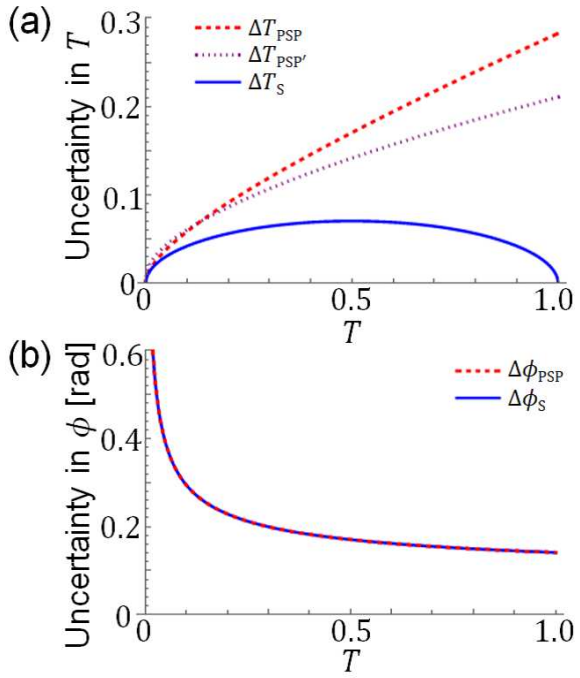

FIG. 3: Measurement uncertainties in the estimation with PSI for $N = 100$ input photons which have a Poisson fluctuation. (a) uncertainties in T. The red dashed curve, the purple dotted curve and the blue solid curve indicate ΔT_{PSP}, $\Delta T_{\mathrm{PSP}'}$ and ΔT_{S}, respectively. (b) uncertainties in ϕ. The red dashed curve and the blue solid curve indicate $\Delta\phi_{\mathrm{PS}}$ and $\Delta\phi_{\mathrm{S}}$, respectively.

IV. CONCLUSION

In conclusion, we have derived the theoretical precision of PSI. We found that the precision of PSI depends on the transmittance and phase for the sample when single photons are input into the interferometer and can be optimized by tuning the second beam splitter of the interferometer. We also showed the trade-off relation between transmittance and phase precision. Then, we compared PSI with SOM. While the transmittance estimation used in standard PSI gives a slightly worse precision than that for SOM, an alternative approach, which is not commonly used in PSI, almost reaches the precision for SOM. Regarding the phase estimation, we found that PSI can achieve a better precision than SOM. We then showed that the phase dependence in the precision disappears when the input photons fluctuate with a Poisson distribution and the precision for the transmittance and phase are inferior to those without Poisson fluctuation. We believe that our results not only open the door to explore sensing and imaging using PSI in the ultra-low light region but also provide the fundamental understanding of precision limit for simultaneous transmittance and phase estimation with photons. It would be interesting to extend the study to quantum-enhanced interferometry [27–30].

ACKNOWLEDGEMENTS

This work is supported by JST-PRESTO (JPMJPR15P4, JPMJPR16P8) and a Grant-in-Aid from JSPS (20H01828, 18K18733, 17H02936).

[1] J. H. Bruning, D. R. Herriott, J. E. Gallagher, D. P. Rosenfeld, A. D. White, and D. J. Brangaccio, Applied Optics **13**, 2693 (1974).
[2] C. Tian and S. Liu, Optics Express **24**, 18695 (2016).
[3] N. Warnasooriya and M. K. Kim, Optics Express **15**, 9239 (2007).

[4] V. Mico, Z. Zalevsky, and J. García, Optics Communications **281**, 4273 (2008).
[5] Z. Wang, L. Millet, M. Mir, H. Ding, S. Unarunotai, J. Rogers, M. U. Gillette, and G. Popescu, Optics Express **19**, 1016 (2011).
[6] Y. Baek, K. Lee, J. Yoon, K. Kim, and Y. Park, Optics Express **24**, 9308 (2016).
[7] Y. K. Park, C. Depeursinge, and G. Popescu, Nature Photonics **12**, 578 (2018).
[8] I. Yamaguchi and T. Zhang, Optics Letters **22**, 1268 (1997).
[9] B. Javidi and E. Tajahuerce, Optics Letters **25**, 610 (2000).
[10] J. Rosen and G. Brooker, Nature Photonics **2**, 190 (2008).
[11] P. Clemente, V. Durán, E. Tajahuerce, V. Torres-Company, and J. Lancis, Physical Review A **86**, 041803(R) (2012).
[12] T. Tahara, R. Mori, S. Kikunaga, Y. Arai, and Y. Takaki, Optics Letters **40**, 2810 (2015).
[13] T. Tahara, R. Mori, Y. Arai, and Y. Takaki, Journal of Optics **17**, 125707 (2015).
[14] Y. Endo, T. Tahara, and R. Okamoto, Applied Optics **58**, G149 (2019).
[15] M. Yamamoto, H. Yamamoto, and Y. Hayasaki, Optics letters **34**, 1081 (2009).
[16] A. Marar and P. Kner, Optics Letters **45**, 591 (2020).
[17] L. Miao, K. Nitta, O. Matoba, and Y. Awatsuji, Applied optics **52**, A131 (2013).
[18] S. Chen and Y. Zhu, Methods **136**, 50 (2018).
[19] M. Sarovar and G. J. Milburn, Journal of Physics A: Mathematical and General **39**, 8487 (2006).
[20] G. Adesso, F. Dell'Anno, S. De Siena, F. Illuminati, and L. A. M. Souza, Physical Review A **79**, 040305(R) (2009).
[21] R. Demkowicz-Dobrzanski, U. Dorner, B. J. Smith, J. S. Lundeen, W. Wasilewski, K. Banaszek, and I. A. Walmsley, Physical Review A **80**, 013825 (2009).
[22] B. L. Higgins, D. W. Berry, S. D. Bartlett, H. M. Wiseman, and G. J. Pryde, Nature **450**, 393 (2007).
[23] R. Okamoto, M. Iefuji, S. Oyama, K. Yamagata, H. Imai, A. Fujiwara, and S. Takeuchi, Physical Review Letters **109**, 130404 (2012).
[24] D. H. Mahler, L. A. Rozema, A. Darabi, C. Ferrie, R. Blume-Kohout, and A. M. Steinberg, Physical Review Letters **111**, 183601 (2013).
[25] K. S. Kravtsov, S. S. Straupe, I. V. Radchenko, N. M. T. Houlsby, F. Huszár, and S. P. Kulik, Physical Review A **87**, 062122 (2013).
[26] R. Okamoto, S. Oyama, K. Yamagata, A. Fujiwara, and S. Takeuchi, Physical Review A **96**, 022124 (2017).
[27] K. Edamatsu, R. Shimizu, and T. Itoh, Physical Review Letters **89**, 213601 (2002).
[28] M. W. Mitchell, J. S. Lundeen, and A. M. Steinberg, Nature **429**, 161 (2004).
[29] T. Nagata, R. Okamoto, J. L. O'Brien, K. Sasaki, and S. Takeuchi, Science **316**, 726 (2007).
[30] R. Okamoto, H. F. Hofmann, T. Nagata, O. J. L., K. Sasaki, and S. Takeuchi, New Journal of Physics **10**, 73033 (2008).